Chapter 3

Sustainable Materials and Biorefinery Chemicals from Agriwastes

M.A. Martin-Luengo, M. Yates, M. Ramos, F. Plou, J. L. Salgado, A. Civantos, J.L. Lacomba, G. Reilly, C. Vervaet, E. Sáez Rojo, A.M. Martínez Serrano, M. Diaz, L. Vega Argomaniz, L. Medina Trujillo, S. Nogales and R. Lozano Pirrongelli

Additional information is available at the end of the chapter

http://dx.doi.org/10.5772/50551

1. Introduction

Countries with economies based on agriculture generate vast amounts of low or null value wastes which may even represent an environmental hazard. In our group, agricultural industrial wastes have been converted into value added liquid substances and materials with several aims: decreasing pollution, giving added value to wastes and working in a sustainable manner in which the wastes of an industry can be used as the raw materials of the same or others, as the "cradle to cradle" philosophy states [1].

Sub-products from the agricultural food industry are being employed as renewable low cost raw materials in the preparation of Ecomaterials, designed for use in a number of industrial processes of great interest. Given their origin, these materials may compete with conventional ones since with this process a sustainable cycle is closed, in which the residues of one industry are used as raw materials in the same or other industries [2].

With regards to the composition of the residues produced from agriculture, the pH of soil is of great importance, since plants can only absorb the minerals that are dissolved in water and pH is mandatory for the physical, chemical and biological properties of soil and the main cause of many agronomic questions related to nutrient assimilation [3-5]. Variations of pH modify the solubility of most elements necessary for the development of crops and also influence the microbian activity of soil, which will affect the transformation of elements that are liberated to the soil and can be assimilated to form crops or not [3]. For example at pH lower than 6 or higher than 8 bacterian activities are lowered, the oxidation of nitrogen to nitrate is reduced and the amount of nitrogen available for plant food is decreased. However Al, Fe and manganese are more soluble at low pHs, reaching even toxic concentrations. Potassium and sulphur are easily adsorbed at pH higher than 6, calcium and magnesium between 7 and 8.5

and iron at pH lower than 6. For alkaline pH in soil, the availability of $H_2PO_4^-$ can be reduced through precipitation of phosphorous containing salts with cations such as calcium Ca^{2+} or magnesium Mg^{2+}. However when soils have acid pH other compounds with HPO_4^{2-} and iron (Fe^{2+}), aluminium (Al^{3+}) and manganese (Mn^{2+}) can form, with increased solubility.

The main factors that influence soil pH are the mineral composition and how it meteorizes, the decomposition of organic matter, how nutrients are partitioned among the solution and aggregates and of course the pluviometry of the zone and atmospheric contamination. Lower pHs are found in places with high pluviometry, with high organic matter decomposition, young soils developed on acid substrates, and places with high atmospheric contamination (acid rain).

Depending on the species, crops can benefit from calcareous soils with high calcium carbonate content such as alfalfa, but other plants prefer soils with acid pH such as potatoes, coffee or tobacco. It is clear that different seasons will produce plants with a varying composition depending on the atmospheric conditions and therefore the materials derived from them need to be characterised and analysed to determine their possible uses.

Variation in content of components in fruits and vegetables depends upon both genetics and environment, including growing conditions, harvest and storage, processing and preparation. For example in broccoli, low soil water content during plant growth and post harvest cold storage were conditions that, combined, gave higher amounts of l-ascorbic acid [6,7]. Higher polyphenol contents are found in organic tomato juices compared to non-organic ones due to a higher phosphorus uptake and limited nitrogen availability in the first case [8]. Therefore, thorough characterisation of the residue composition is a key step before determination of the possible uses of a given residue.

Among the applications being developed in our group, Bio-refinery processes (preparation of sustainable *p*-cymene and hydrogen, avoiding the use of petroleum derivatives and synthesis of pharmaceutical and fine chemical intermediates), design of structured materials capable of effluent decontamination and preparation of biomaterials to act as scaffolds for cell growth towards development of prostheses and implants, will be considered here.

Given its multidisciplinary approach, this work is being carried out through the collaboration among national (Institute of Materials Science of Madrid (ICMM, CSIC), Institute of Catalysis (ICP, CSIC), Centre of Molecular Biology Severo Ochoa (UAM-CSIC), Polytechnic University of Madrid (UPM), University at distance (UNED), University Complutense of Madrid (UPM) and international (University of Sheffield and University of Ghent) research groups, in addition to various industries interested in the transformation of their residues and or sub-products into "value added materials", with whom various research projects have been and are being sponsored by the MICINN and CDTI.

2. Production of sustainable *p*-cymene and hydrogen

Environmental problems pose a great challenge, particularly in countries such as Spain, where water use, residues desertic and contaminated soils have become a matter of the

utmost concern. Efforts from academia, industry and government are mainly based on technological changes that improve chemical processes to avoid negative environmental consequences. New renewable and sustainable chemicals are now being obtained from agricultural wastes, applying "biorefinery technologies", which reduce the need for non-renewable fossil fuel resources to help solve many environmental problems. Spain is the third producer of citrus fruits in the world [9]. Limonene is a six membered ring terpene, present in agricultural wastes derived from citrus peels, with a purity of more than 95% in orange peel oil. Sustainable *p*-cymene and hydrogen were prepared form limonene, comparing commercial and agricultural waste derived catalysts and conventional and non-conventional activation paths. These studies show interesting results through the development of solids that activate certain kinds of reactions shown in Figure 1.

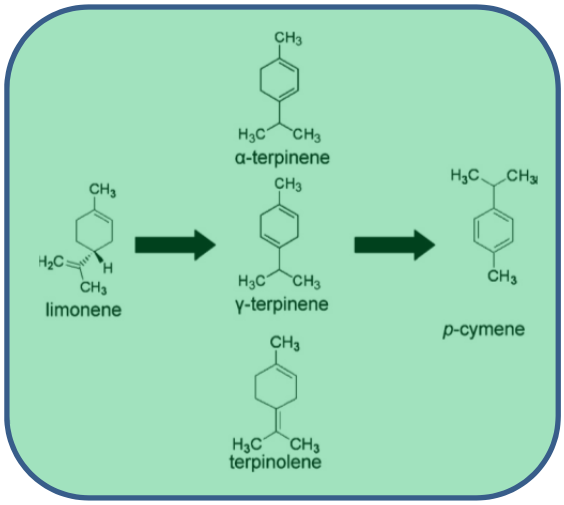

Figure 1. Conversion of limonene to *p*-cymene and reaction intermediates

This work is based on designing a clean process to transform limonene, into *p*-cymene, in a rapid, simple and economic way. Limonene, a cyclic terpene with empiric formula $C_{10}H_{16}$, is extracted with a purity of *ca*. 95% from citrus fruit processing. Although initially used in pharmaceutical industries, food is the main means for human exposure, although due to its low toxicity [10] it does not constitute a risk to human health at the actual exposure levels. This compound has various uses, as a biodegradable solvent for resins (replacing organic solvents such as mineral oils, methyl-ethyl ketone, toluene, glycolic ethers, CFCs, or as an additive in pigments, inks and adhesives. However, new uses are being sought to give added value to this subproduct, thus increasing the income of these industries, but also with an obvious benefit to society. From the chemical structure of limonene, shown in Figure 1, it may be appreciated that having a six membered ring this substance has the potential to obtain compounds that are usually produced employing petroleum derivatives, with the added bonus of it being a less toxic renewable intermediate. In this study the production of *p*-cymene, an important intermediate in industrial fine chemicals syntheses, for fragrances,

flavourings, herbicides, pharaceuticals, *p*-cresol production, syntheses of not nitrated musk's (i.e. tonalide), etc. [11] will be described.

The preparation of *p*-cymene is usually carried out by Friedel-Crafts alkylation of toxic benzene or toluene (from petroleum), with $AlCl_3$ as catalyst and the respective halides or propanol [12]. In these processes mixtures of *ortho* and *para* isomers, are found and therefore further separation processes are required. Furthermore, the use of benzene or toluene and $AlCl_3$ are restricted by environmental legislation in industrialised countries. In this study a series of commercial silica–alumina mixed oxides, supplied by Sasol, with silica contents ranging from 1 to 40 wt.% designated as SIRAL 1 to SIRAL 40, accordingly, were employed. The textural and acid characteristics of these materials were determined and related with their catalytic activities in the transformation of limonene to *p*-cymene using microwave irradiation as a rapid and efficient energy source, alternative to conventional heating, where apart from the advantage of substantially reduced reaction times the product selectivity was also enhanced [10].

The texture of the mixed oxides: surface areas and pore volumes were analysed by nitrogen adsorption/desorption isotherms at −196°C, in a Tristar apparatus from Micromeritics, on samples previously outgassed at 300°C to a vacuum of less than 10^{-4} torr to ensure that they were clean, dry and free from any loosely adsorbed species. The BET method was used to determine the specific surface areas (S_{BET}) from the adsorption data in the relative pressure range of 0.05–0.30 $p/p°$ and the mesopore size distributions were calculated from the desorption branch of the nitrogen isotherm using the Kelvin equation and the BJH method with the parameters for the thickness of the adsorbed layers from the Harkins–Jura equation, chosen since this employed a metal oxide as the non-porous standard [13].

The acidities of the solids were analysed from their ammonia adsorption capacities, determined on a Micromeritics ASAP 2010 device, after being outgassed overnight at 300°C to a vacuum of $>10^{-4}$ torr, then the ammonia adsorption isotherms at 30°C were determined up to a pressure of about 350 torr, obtaining the total chemisorption plus physisorption capacities. Subsequently the sample was outgassing at 30°C and a second adsorption isotherm at 30°C determined to measure the physisorption capacity of the sample. The chemisorption capacity was calculated from the differences in the ammonia uptakes between the first and second isotherms. The total acidities were subsequently calculated assuming that each molecule of ammonia reacted with one acid site [14].

Pyridine adsorption coupled with infrared analysis was used to qualitatively determine the Lewis (Al^{3+}) and Brønsted (Al-OH) acid sites of the materials, these being capable of catalysing the conversion of limonene to *p*-cymene. The catalysts were pressed as self-supporting discs, outgassed under high vacuum, contacted with pyridine vapour and outgassed to obtain the infrared spectra corresponding to Lewis and Brønsted acid sites with adsorption peaks at 1455 and 1545 cm^{-1}, respectively [15]. The microwave reactions were carried out with a programmable focalised monomodal microwave apparatus, Synthewave 402 from Prolabo, under both dry media and reflux conditions. Dry media microwave induced reactions can be considered a clean technology, since no solvents are

used. In those experiments 50 μl of limonene were physically mixed with 200 mg of solid, placed in a glass reactor and irradiated at 300 W for 5, 10 or 20 min. In reflux conditions 500 mg of solid was mixed with 5 ml of limonene and heated with a reflux column to 165°C for 10 or 20 min, avoiding overheating of the reaction mixture. The final temperature was chosen to be slightly lower than the boiling points of the reactant and products (limonene 175°C, *p*-cymene 177°C) in order to control the reaction. At the end of the experiments the reaction mixtures were cooled, extracted and dissolved in ethanol and analysed by gas chromatography coupled to a mass spectrometer (GC–MS). Following the extraction of the reaction products with ethanol, the catalytic activities of the samples were redetermined to ascertain if the materials had suffered any change in their activities or selectivities.

It has been previously proposed that the available surface area coupled with the accessibility to the active acid sites play important roles in controlling the catalytic process in this reaction [16]. The specific surface areas, pore volumes and average mesopore diameters of the solids are summarised in Table 1. The nitrogen adsorption/desorption isotherm for SIRAL 1 was of type IV with a well-defined plateau at high relative pressures with a type H1 hysteresis loop, characteristic of a mesoporous solid with a narrow well defined mesopore size distribution [13]. On increasing the silica content the specific surface area, mesopore volume and average mesopore diameters increased progressively as evidenced by a widening of the hysteresis loop between the adsorption and desorption branches and with the highest silica contents the plateau at high relative pressure became less well defined as the pore sizes shifted into the narrow macropore range. From the isotherms obtained for SIRAL 1 and SIRAL 40 presented in Figure 2 the change in the hysteresis loop due to the widening of the pores may be appreciated while the upward displacement of the curve with the increased silica content was indicative of the greater specific surface area. The other samples with intermediate silica contents, not shown here for clarity, gave rise to adsorption/desorption curves that lay between these two extremes.

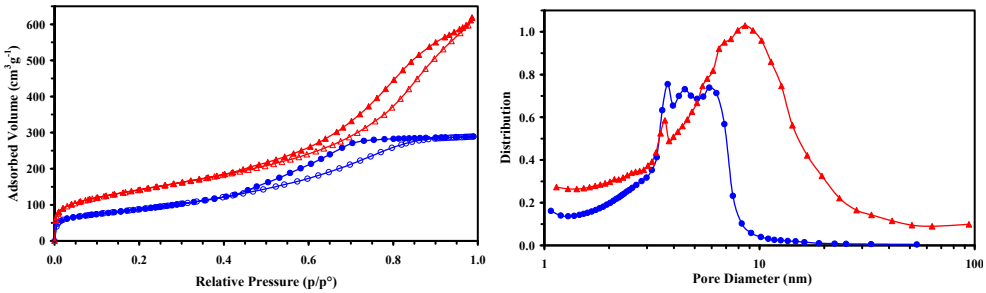

Figure 2. Textural characteristics of mixed oxides SIRAL 1 ○● and SIRAL 40 Δ▲

Since the reaction is catalysed by the acid sites, the higher activity as the number and accessibility of the surface acid sites rose with increased silica content was to be expected. Greater activities were found as the total acidity was increased (measured by ammonia adsorption, shown in Figure 3).

Sample	Surface area (m^2g^{-1})	Pore volume (cm^3g^{-1})	Average mesopore diameters (nm)	
SIRAL 1	321	0.45	4.5	5.8
SIRAL 5	364	0.57	4.8	5.9
SIRAL 10	422	0.59	4.8	6.8
SIRAL 20	432	0.68	5.4	9.4
SIRAL 40	506	0.95	5.8	12.7

Table 1. Textural properties of the mixed oxides

The catalytic activity results obtained with microwave irradiation of limonene are presented in Table 2.

		Selectivity				
Sample	Time (min)	Conversion (%)	α-terpinene (%)	*Γ-terpinene* (%)	*α –terpinolene* (%)	*p*-cymene (%)
	5	15	85	0	15	0
SIRAL 1	10	56	52	14	0	34
	20	100	0	0	0	100
	5	42	60	12	21	7
SIRAL 5	10	63	27	25	0	48
	20	100	0	0	0	100
	5	65	48	11	31	10
SIRAL 10	10	69	15	0	14	71
	20	100	0	0	0	100
	5	88	31	6	15	48
SIRAL 20	10	100	0	0	0	100
	20	100	0	0	0	100
	5	93	0	0	3	87
SIRAL 40	10	100	0	0	0	100
	20	100	0	0	0	100

Table 2. Limonene conversions and selectivities under dry media conditions

During the reactions (SIRAL 1 shown as example in Figure 4), only α-terpinene, γ-terpinene, γ-terpinolene (from isomerisation) and *p*-cymene (from dehydrogenation) were found as products, with no other compounds such as menthanes or menthenes, produced by disproportionation or polymerisation, detected. In Table 2 it should be noted that the selectivity to *p*-cymene increased with both longer irradiation times and increased silica contents. For the two samples with the highest silica contents reaction times of just 10 min

gave selectivities to *p*-cymene of greater than 90%. Since these samples had the most acid centres, calculated on both per gram or per m^2g^{-1} basis, it would appear that the selectivity to *p*-cymene was due to the rapid aromatisation of the intermediates produced by isomerisation over the acid centres. Although conversion of limonene to *p*-cymene over Lewis acid sites with conventional heating is known, the much longer reaction times necessary to increase the overall conversion (3 h) leads to reduced selectivities due to the formation of undesirable mentanes, etc. [17].

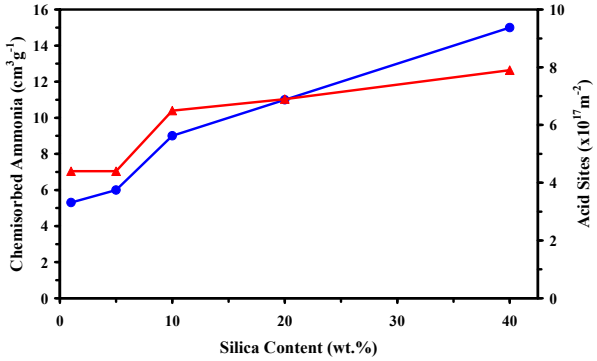

Figure 3. Ammonia chemisorption cm^3g^{-1} ● and number of acid sites m^{-2} ▲ vs. silica content of the mixed oxides.

In order to carry out the reaction in conditions similar to those used industrially the two samples with the highest activities in dry media were chosen for further study in reflux conditions, with the ratio between the reactants and the solid: 0.00025 and 0.01 cm^3g^{-1}, respectively. From Table 3 it may be observed that the intermediate isomerisation product *α*-terpinene was only found for SIRAL 20 and at a very low level (4%) and 100% conversion of limonene to *p*-cymene was achieved with Siral 40 after 10 min. The speed of the reaction when heated by microwave irradiation is possibly the reason for the high selectivities, since the short reaction time necessary to attain these high conversions and selectivity to *p*-cymene avoid the formation of undesirable by-products such as mentanes (products of disproportionation) or polymers, that are found with the longer reaction times employed with conventional heating [18]. Thus, microwave irradiation favoured the production of *p*-cymene from limonene, avoided the use of highly toxic benzene, toluene and aluminium trichloride and allowed high conversions and excellent selectivities towards the desired product due to the accelerated reaction rates. As the reaction is governed by the number and accessibility of the acid sites greater activities were achieved with increased silica contents, which led to higher specific surface areas, pore volumes and average pore sizes in addition to an increased number of acid sites.

2.1. Modified clays

Sepiolite modified with sodium hydroxide and impregnated with either iron or manganese salts were also used as catalytic supports for conversion of limonene to *p*-cymene. The use of

an inexpensive natural clay for the catalyst preparations reduces costs and the need for commercial synthesised solids is avoided. The sepiolite used was from Tolsa SA (hydrated magnesium silicate of the philosilicate type 2:1 with a layer of magnesium between two layers of silica tetrahedra. The octahedral sheet is composed mainly of Mg^{2+}, mainly composed of SiO_2, 62%, MgO 25%, Al_2O_3 1.2%, Fe_2O_3 0.5%). This natural clay of high abundance in Madrid (Spain), has a specific surface area (S_{BET}) close to 300 m^2g^{-1}, of which 150 m^2g^{-1} is external (pores with diameters >2 nm ø) and the rest is due to the micropores of the material (< 2nm). It has a high density of –SiOH groups originated at the edges due to breakage of Si-O-Si bonds at *ca.* 0.5 nm intervals, having a density of *ca.* 2.2 groups/10 nm^2[19].

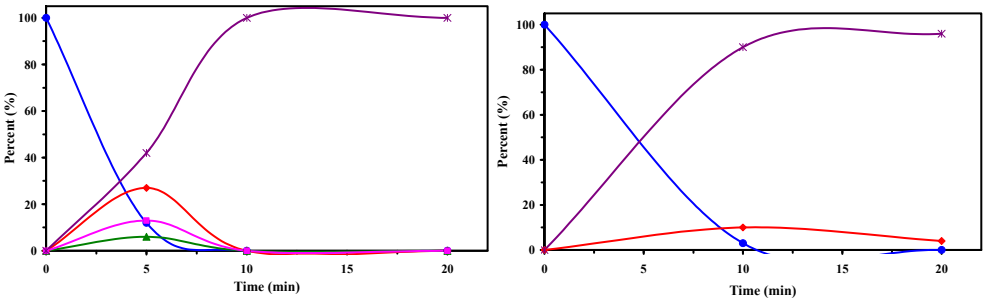

Figure 4. Reactant and product distributions vs. time for (a) Siral 1 in dry media and (b) Siral 20 under reflux: limonene (●), α-terpinene (♦), γ-terpine (▲), α-terpinolene (■) and *p*-cymene (✳)

The activity of the parent sepiolite was modified by adding 5.75 wt.% of iron or manganese, in the form of their nitrate or acetate, respectively, since their oxides efficiently absorb microwave radiation and have low toxicity compared to other metals commonly used as catalysts (*i.e.* Pd, Cd, Cr etc.), or price (Au or Ag). A further sample was pretreated with sodium hydroxide to introduce a similar amount of sodium.

The best procedure to decompose the impregnated compounds to their corresponding supported oxides was determined with TG-DTA analyses in air flow of the precursors in a Stanton model STA 781 thermogravimetric analyser up to 1000ºC. The thermograms obtained show 8% loss of adsorbed water in the interval 20-120ºC, 5% at 120-250ºC loss of sepiolite (zeolitic) water, and 8% loss for decomposition of the anions at *ca.* 400ºC for iron nitrate and at ca. 300ºC for the manganese acetate. In accordance with these findings all the precursor solids were calcined at 400ºC for 4 h in a 50 cm^3min^{-1} air flow [20].

The nitrogen adsorption isotherms for the parent sepiolite heat treated at 400°C gave a mixed type I/II form, due to the presence of both micropores (0-2 nm) and mesopores (2-50 nm) that extend into the macropore region (> 50 nm). For the SepFe (Figure 5), SepMn and SepNa there was a loss in the specific surface area due to the collapse of the microporous structure of sepiolite by folding due to the thermal treatment. For all samples the hysteresis loops were of type H3, typical for solids with slit-shaped pores, commonly found with clay materials.

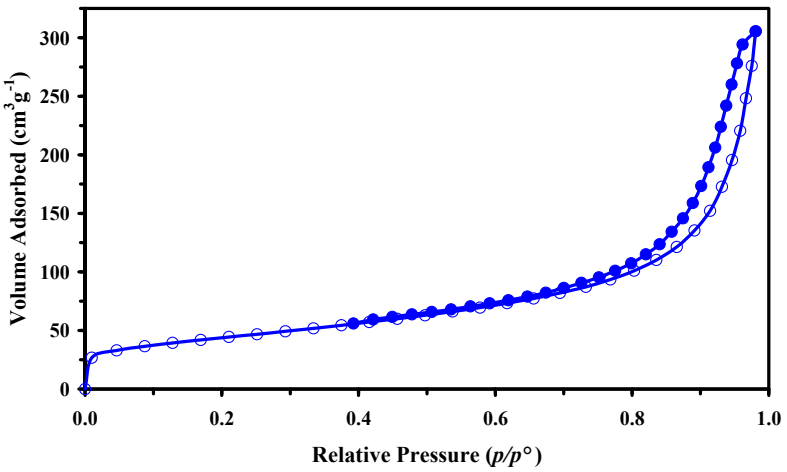

Figure 5. Nitrogen isotherm for SepFe

Sample SepNa had the lowest pore volume and surface area, probably due to blocking of pores with sodium species. The textural data from the corresponding isotherms are presented in Table 3.

Solid	S_{BET}	S_{EXT}	V_{mic}	V_{mes}	V_t
Sepiolite	298	149	0.038	0.417	0.455
SepNa	100	93	0.002	0.362	0.364
SepFe	155	149	0.002	0.416	0.418
SepMn	153	138	0.008	0.431	0.439

S_{BET} = Specific surface area (m^2g^{-1}) S_{EXT} = External surface area (m^2g^{-1}) Vmic = Micropore volume (0-2nm pore diameter, cm^3g^{-1}), V_{mes} = Mesopore volume (2-50nm pore diameter, cm^3g^{-1}), Vt = Total pore volume (cm^3g^{-1}).

Table 3. Textural characteristics of the solids

A JEOL model FXII electron microscope operating at 200kV was used to study the structure of the materials. The basic sites of the solids were quantified by the adsorption-desorption of carbon dioxide in a Coulter Omnisorp 100 apparatus on solids previously outgassed to clean the surface at different temperatures to quantify the amount and strength of basic sites. The results obtained by this procedure are included in Figure 5 [21].Transmission electron microscopy showed the oxide particles present in the structures of SepFe and SepMn with sizes of 4-5 nm but with no other observable alteration to the fibrilar sepiolite structure and a more homogeneous distribution of the oxide particles for SepFe compared to SepMn, which reduce the exposed oxide area during reaction compared to SepFe. Homogeneous particle sizes have been claimed to be a positive effect for the reactivity in these kinds of reactions.

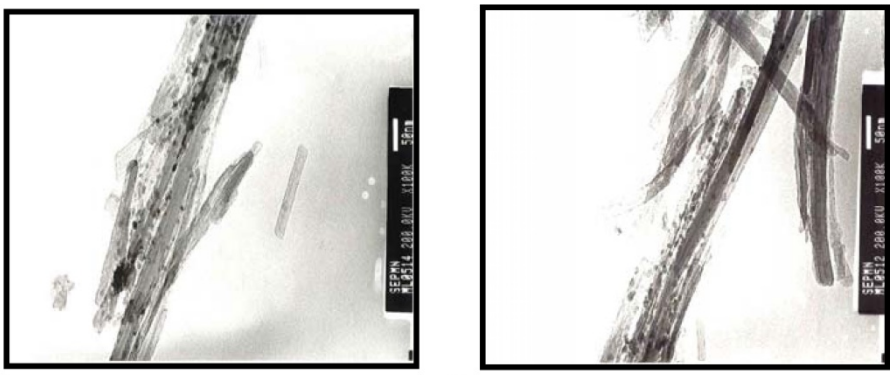

Figure 6. Transmission electron micrographs of (a) SepMn and (b)SepFe.

The amount and strength of acid sites determined by TPD of pyridine (Figure 7) showed the measured acidities followed the order: SepFe > SepMn > Sep. As expected no pyridine adsorption was found for the sample pretreated with sodium hydroxide (SepNa). The increase in the amount and strength of acid sites by addition of iron or manganese oxides to these supports was mainly related to the presence of Fe^{x+} and Mn^{x+} ions (Lewis acidity) and to surface OH groups (Brönsted acidity) [22].

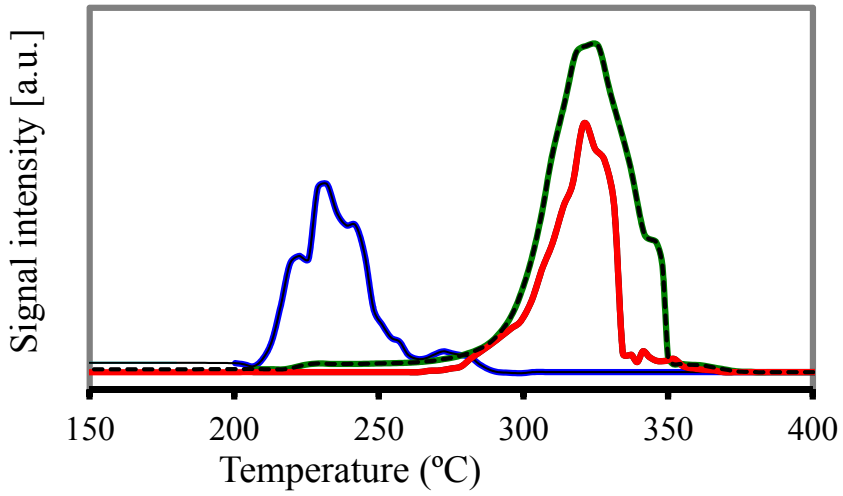

Figure 7. Pyridine determination of acid sites on Sepiolite, SepMn and SepFe.

From the adsorption-desorption of carbon dioxide shown in Figure 8 the basicity of Sepiolite (due to the existence of basic sites mainly Mg^{2+} ions and oxygen on the surface) is low, while temperatures in excess of 400ºC were needed to desorb carbon dioxide from the other three materials. The solid with greater amount of stronger basic sites was SepNa. Samples SepFe

and SepMn were more basic than Sepiolite and had greater total amounts of basic sites of lower strength.

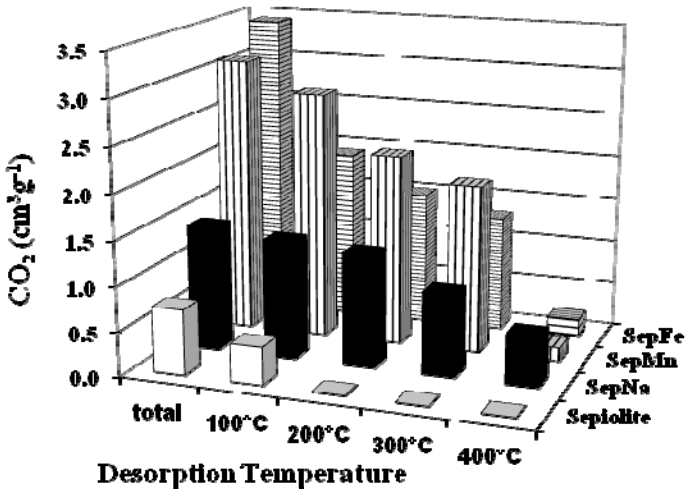

Figure 8. Basicity of the catalysts by CO_2 adsorption-desorption

For the reactions under dry media (200 mg of catalyst mixed with 0.057 ml of limonene) and solvent free conditions, after irradiation the system was cooled and eluted with 2 ml ethanol and filtered to extract the reactants and products and subsequently analysed as described in section 1.1. In the solvent free reactions, a temperature of 165ºC, was chosen to transform limonene, based on the results obtained under dry media conditions. In this case 5 ml of limonene and 500 mg of catalyst were used and a reflux attachment included in the microwave oven. At the end of the experiment 0.057 ml of liquid were dissolved in 2 ml of ethanol to follow the analysis procedure as described above. The results for the dry media reactions are shown in Table 4.

Sample	Reaction Time (Min)	Conversion (%)	Product Distribution (%)			
			α-terpinene	γ-terpinene	α-terpinolene	*p*-cymene
Sepiolite	5	35	25	8	31	36
	10	73	26	0	0	74
	20	100	0	0	0	100
SepFe	5	75	0	0	0	100
	10	100	0	0	0	100
	20	100	0	0	0	100
	5	89	0	0	0	100

Sample	Reaction Time (Min)	Conversion (%)	Product Distribution (%)			
			α-terpinene	γ-terpinene	α-terpinolene	*p*-cymene
SepMn	10	100	0	0	0	100
	20	100	0	0	0	100

Table 4. Conversions and selectivities under dry media conditions

SepNa did not show activity, with high amounts of basic sites and practically non-existent acid sites, even though it reached the highest temperature during microwave heating. With sepiolite, selectivity to *p*-cymene rose, reaching 100% after 20 min and for SepFe and SepMn after only 10 min due to iron or manganese that are microwave adsorbing centres compared to the parent sepiolite, but not to the final temperature attained (Figure 9).

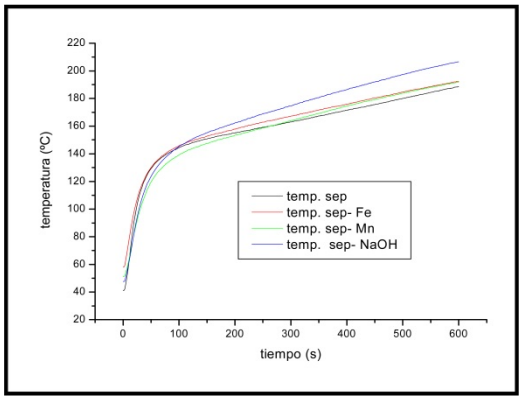

Figure 9. Temperatures reached under dry media conditions

The solids that presented activity under dry media conditions (Sepiolite, SepFe and SepMn) were tested in the liquid phase reactions that allow higher liquid to solid ratios (Table 5) and the temperatures reached are included in Figure 10.

Sample	Reaction Time (Min)	Conversion (%)	Product Distribution (%)			
			α-terpinene	γ-terpinene	α-terpinolene	*p*-cymene
Sepiolite	10	100	0	0	0	100
	20	100	0	0	0	100
SepFe	10	85	32	19	35	14
	20	100	9	3	0	88
SepMn	10	10	34	8	58	0
	20	75	33	17	33	17

Table 5. Conversions and selectivities in liquid phase

As in dry media, the selectivity to *p*-cymene increased with longer reaction times and higher temperatures, in agreement with the fact that the formation of this product is an endothermic reaction. Under these reaction conditions Sepiolite gave the best results for both activity and selectivity, reaching 100% conversion and selectivity after only 10 minutes. The differences in the temperature profiles for these three materials during the reaction, were not so great as to explain such differences in their catalytic activities and selectivities.

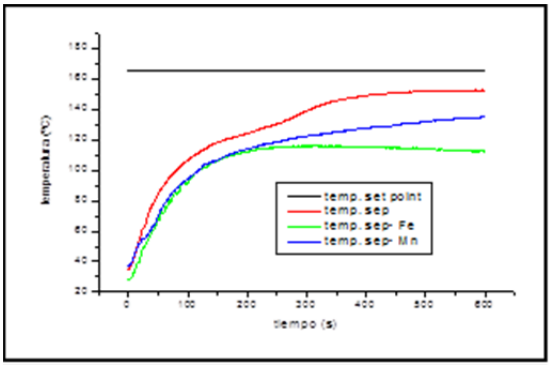

Figure 10. Temperatures reached under solvent free conditions.

The strong basic sites present in SepNa, SepMn and SepFe may be capable of adsorbing limonene to such an extent that it was not readily available for reaction under the reaction conditions, this being the reason why Sepiolite is the most active solid for the dehydrogenation of limonene to *p*-cymene. Previous work by the authors showed that the acid sites of silica–alumina mixed oxides could dehydrogenate limonene in conditions similar to those used here [10]. Thus, the acid sites present on the Sepiolite surface, although weaker than those found with iron or manganese containing solids, were of the right strength to convert limonene to *p*-cymene. Further experiments showed that 300 mg of Sepiolite were enough to convert 5 ml of limonene to *p*-cymene in 10 min with a 100% conversion and selectivity. Similar conversions and selectivities to those found in this study have recently been reported for the transformation of limonene, although dangerously high hydrogen pressures, greater than atmospheric and the use of toxic and expensive palladium catalysts were required [23].

Conventional heating of limonene using acid solids as catalysts in liquid-solid conditions leads to lower activities and selectivities than those found in this work. We believe the short reaction times required using dielectric heating were responsible for the higher conversions and selectivities, due to the increased activity of these paramagnetic absorbing centres, thus avoiding other products such as dimers and polymers, that are formed during the longer reaction times necessary with conventional heating [17].

3. Sustainable fine chemicals from agri wastes

A vast amount of work has been carried out regarding the preparation of fine chemicals, with oxidation being one of the main paths followed. Renewable value added chemicals

were prepared in this work using solid and liquid agricultural industrial wastes from rice and citrus production, as renewable raw materials, avoiding the use of substances toxic to the environment and achieving a reduction in energy expenditure. The whole process is consistent with a sustainable development. The present investigation has demonstrated how the transformation of a low value subproduct (limonene) into high value materials (carvona, carveol and limonene epoxides) can be achieved with similar conversions and selectivities to those found in the literature for catalysts that have higher toxicity and are less environmentally friendly.

After a thorough review of literature data, careful design of oxidation conditions of limonene allows the production of carvone and carveol through allylic oxidation and limonene oxides through double bond epoxidation (Figure 11). These products have interesting pharmaceutical properties and also are chemical intermediates with prices from 5 to 10 times higher than limonene [9].

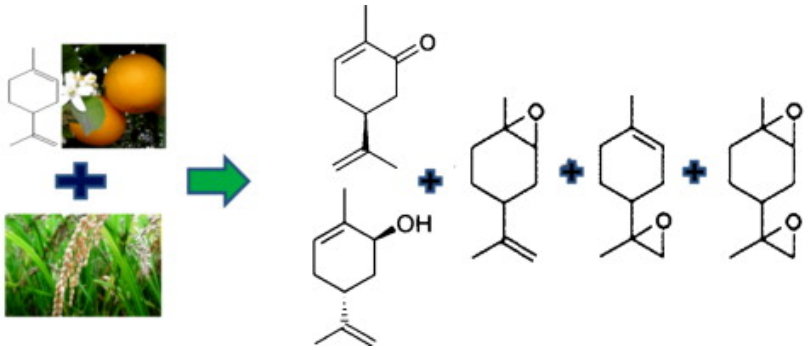

Figure 11. Renewable carvone, carveol and epoxides prepared from limonene. Source of photographs: http://www.finecooking.com/assets/uploads/posts/5552/ING-oranges_sql.jpg http://1.bp.blogspot.com/_siEMqPzFQAY/TJO2Pt4tX3I/AAAAAAAABW0/gWJ_-7IP9co/s1600/arroz9.jpg

A clean process for this transformation was developed here by using iron oxide supported on silica (RHS) from rice husk (RH) to catalyse the reaction. RH is produced in huge amounts annually and its ash contains *ca*. 94% silica, with the added bonus of zero CO_2 energy being produced during the calcination of RH to produce RHS.

The organic reactions carried out in this work were activated with dielectric heating that allows higher yields under mild reaction conditions, avoiding thermal decomposition of sensitive products or reagents, and therefore affecting selectivity [10]. Tert-butyl hydroperoxide (tBHP) was used as oxidant due to its easy handling characteristics and high thermal stability. The tert-butanol and its by-products on oxidation, can be distilled and recycled, a particularly important step when industrial amounts are required. Silica from rice husk (RHS) was used as support and catalyst. It was prepared by calcining rice husk in air at 500°C for 4 h. For comparison reasons, silica Aerosil Evonik was used since it had similar textural properties to RHS (surface area of 91 m^2g^{-1}). The supported catalysts

were prepared by dry impregnation of RHS with iron nitrate ($Fe(NO_3)_3 \bullet 9H_2O$ (> 99% purity, Sigma-Aldrich) solutions, the impregnated precursors were air dried overnight at 100ºC, prior to TG-DTA and FTIR studies of the calcination procedures necessary to produce FeOx/RHS catalysts (400 or 600ºC, 4 h in air). Since treating silica with low pH iron nitrate solutions can produce structural changes, fresh RHS was treated with nitric acid solutions of the impregnating pH (1.4) and then calcined at 400 or 600ºC, for comparison purposes

The basicity of the solids was measured by decomposition of acetic acid, in a gas analysis system with quadrupole mass spectrometry, model M3 QMS200 Thermostar coupled to a thermogravimetric/differential thermal analysis equipment, Stanton STA model 781. Increasing the temperature of the spiked solids under nitrogen flow at a heating rate of $5ºCmin^{-1}$ up to 700ºC, recording the evolution of mass 44, ascribed to CO_2. The amount and temperature of evolution of the CO_2 signal gave an indication of the strength and amount of basic sites. The CO_2 signal was calibrated from the decomposition of a known amount of calcium oxalate.

The catalytic oxidations of limonene were studied in a programmable focussed microwave oven Syn402 from Prolabo, described above in section 1.1. Preliminary experiments were carried out in dry media conditions on the Fe-containing catalysts, to determine the best conditions to use in further liquid/solid experiments, choosing the conversion of limonene and selectivity to carvone as parameters for comparison of the effects caused by the various conditions studied. Studied parameters were the limonene: tBHP volume ratio, temperature and reaction time. Based on these preliminary experiments, the conditions chosen for the liquid phase work were 300W microwave power, with a reflux attachment, reaction temperature (150ºC) and reaction time up to 120 min, using 4 ml limonene, 14 ml of TBHP solution and 150 mg of catalyst. Conventional heating results were carried out for comparison with similar amounts of reactants and catalyst, starting the reaction time from the moment the reaction temperature was reached and the catalyst added. The effects of reaction temperature, amount of catalyst and oxidant on both the reactivity and selectivity were studied using the most promising catalyst. The reactants and products were analysed in a GC-MS system, as described above.

The chemical composition of the RHS used in this work was 6% S, 2% K, 1% Cl, P and Ca, 0.1% Mn and Fe and 0.04% Zn. The iron containing precursors were calcined at 400 or 600ºC for 4 h, according to TG-DTA and FTIR data. The iron containing catalysts (FeO_x/RHS) had 4.8% or 8.9% Fe. XRD patterns indicated the amorphous nature of RHS and the FeOx/RHS show crystalline iron oxide particles, more common on increasing the amount of iron and calcination temperature, due to sintering, corresponding to maghemite (γ-Fe_2O_3: 36º, 44º, 54º, 58º and 63º) and hematite (α-Fe_2O_3: 24º, 33º, 36º, 50º and 62.5º).

Textural analyses gave rise to the results included in Table 6, showing nitrogen isotherms of type IIb with hysteresis loops type H3, typical of samples with slit-shaped mesopores that extended into the macropore region, caused by the spaces between the plates of material and with no microporosity according to the t-plot analyses [13]. It may be observed that

higher calcination temperatures caused a fall in the surface area and a shift in the hysteresis loop to higher relative pressure/wider pores, due to sintering of the samples, in agreement with XRD results.

Solid calc. T ºC	S_{BET}/m^2g^{-1}	V_{mes}/mLg^{-1}
RHS	85	0.172
RHS HNO_3 400	93	0.203
RHS HNO_3 600	93	0.210
4.8%Fe/RHS 400	118	0.200
4.8%Fe/RHS 600	92	0.185
8.9%Fe/RHS 400	122	0.181
8.9%Fe/RHS 600	87	0.163

Table 6. Textural analyses of catalysts

Most silicas are almost transparent under the electron beam of the transmission microscope and therefore easy to distinguish from oxide particles deposited on their surfaces [24]. However, the RHS particles prepared in this work showed an unexpected dense structure under study by TEM and SEM (Figure 12), formed by lamellar entities, in agreement with the shapes of the nitrogen isotherms, explained above, that made it difficult to distinguish the iron oxide particles.

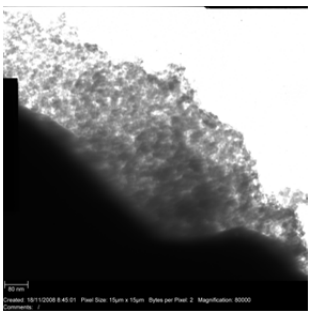

(a) Scale bar: 80 nm

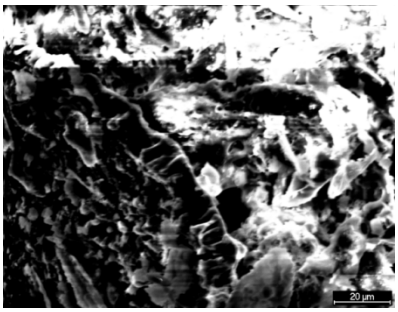

(b) Scale bar: 20 µm

Figure 12. Electron micrographs for 8.9% Fe/RHS 400 a. TEM b. SEM

The adsorption of acetic acid used to characterise the catalysts basic sites produces mainly carbonate, bidentate or bridged acetate species, that decompose to CO_2, giving rise to bands due to the interaction with basic centres of higher basicity with increasing temperature, i.e. T< 150ºC for the desorption of physically adsorbed CO_2, those at T = 150-250ºC corresponding to molecules of CO_2 evolved from basic sites of low to medium strength, whilst those at T = 300-400ºC correspond to the interaction with basic sites of medium to high strength (Figure 13)[25]

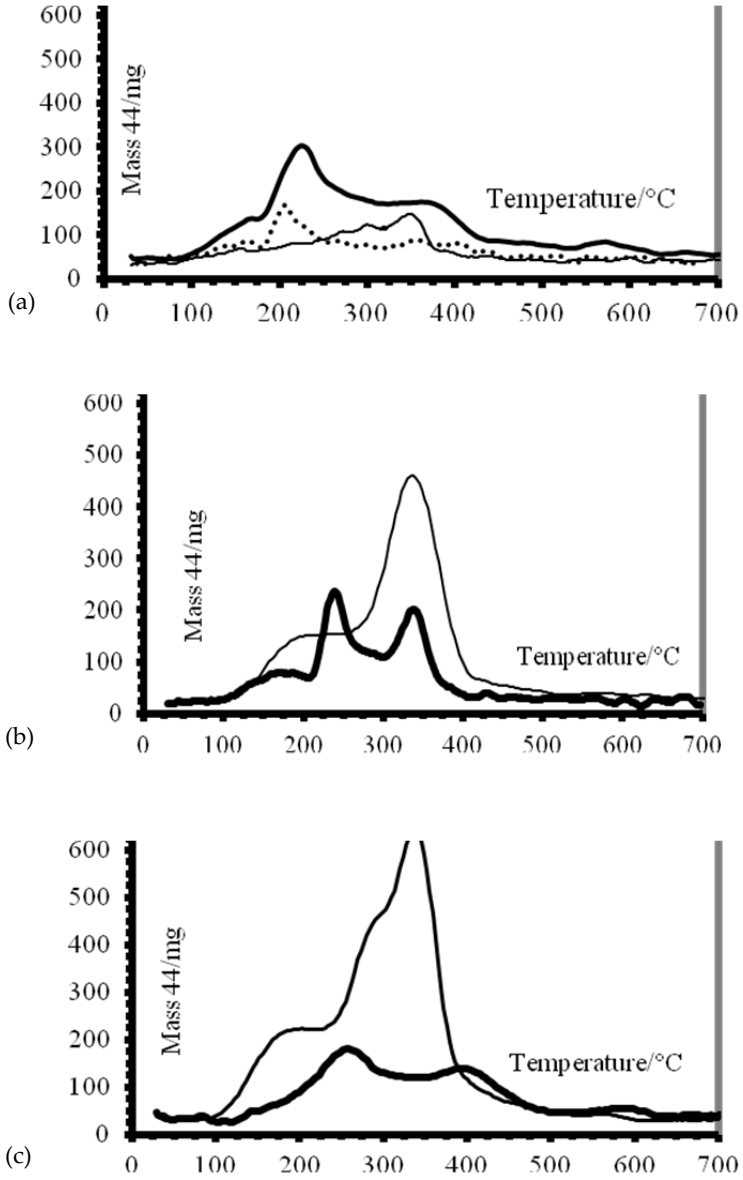

Figure 13. Mass 44/mg evolved from acetic acid decomposition on:
4a. Original and modified RHS (dotted line: RHS, thick line RHS HNO_3 400, thin line RHS HNO_3 600)
4b. 8.9%Fe/RHS (thick line calcined at 600ºC, thin line calcined at 400 ºC)
4c. 4.8%Fe/RHS (thick line calcined at 600ºC thin line calcined at 400 ºC)

From these data it was concluded that the materials employed had the following order of basicity:

Silica Evonik <<< RHS HNO_3 600 < RHS < RHS HNO_3 400

The traces obtained with silica Evonik were within the noise level of the technique, indicating that the acetic acid was only physisorbed, due to its low basicity. These results can be explained taking into account that the basicity, related to both the strength and number of basic sites of RHS was mainly due to the presence of basic oxides. On treating RHS with nitric acid, particles are disaggregated leading to an increase of basic sites available on the surface, but at higher calcination temperatures sintering of the particles occurs decreasing the amount of surface basic centres. The Fe-containing catalysts present higher basicities than the RHS due to the presence of iron oxide, but those calcined at 600ºC have lower basicity than their analogues calcined at 400ºC, in agreement with the sintering occurring in the particles of iron oxide, XRD, textural and published data [26].

Epoxidation and allylic oxidation reaction pathways of limonene are competitive, with valuable epoxides, carvone and carveol being produced. The selective oxidation of alkenes in the presence of peroxides and basic site containing materials is advantageous, since epoxides undergo breakage on acid sites, which decreases the selectivity of the processes. A thorough analysis of literature on limonene oxidative transformations data provide an insight into the conditions needed to convert limonene into value added and renewable limonene oxides (mono or diepoxides) from epoxidation through electrophilic attack at the double bonds, and allylic oxidation when hydrogen abstraction is the dominant reaction towards carvone and carveol, both interesting molecules, since they retain the olefinic functionality, which allows further useful transformations [27, 28].

The catalytic activity was first measured under dry media conditions, reacting 150 mg of catalysts and 48 μL of limonene:tBHP solution, with different limonene:tBHP volume ratios and temperatures, in order to determine optimal conditions for further liquid phase reactions, that allow treating higher amounts of limonene. Experiments with no control of solid temperature and times over 20 min produced evaporation of reactants, giving rise to irreproducible results, which were avoided by maintaining the temperature of the solid constant throughout the reaction, leaving the microwave power to vary accordingly and limiting the reaction times to 20 min. Under these conditions, the experiments were carried out in duplicate and the results obtained with the Fe-containing catalysts under dry media conditions at 120ºC and 20 min irradiation time, with limonene:tBHP solution= 1:1 (volume ratios) are included in Table 7, showing that under equal conditions, the best catalyst for conversion and selectivity to carvone was 8.9%Fe/RHS 400. The catalysts with higher iron content and lower calcination temperatures present higher activities although the selectivities were similar for catalysts with similar iron contents.

With other reaction variables maintained constant, Table 8 shows that by increasing the amount of oxidant the conversion of limonene increases, but that at high amounts the selectivity to carvone starts to decrease and the more oxidised product carvacrol was found. From these results an optimum limonene:tBHP solution=1:3.5 (volume ratio) was chosen.

Catalyst	Conversion (%)	$S_{carvone}$ (%)
No catalyst	0	
4.8%Fe/RHS 400	35	35
4.8%Fe/RHS 600	25	36
8.9%Fe /RHS 400	48	45
8.9%Fe/RHS 600	39	48

S = selectivity

Table 7. Conversions and selectivities of Fe-containing catalysts under dry media conditions (limonene:tBHP ratio=1:1, 120ºC, 20 min, free microwave power, 0.15 mg catalyst)

Limonene:tBHP solution	Conversion (%)	$S_{carvone}$ (%)
1:1	48	45
1:2	55	37
1:4	63	23
1:3.5	60	36

Table 8. Conversions and selectivities of 8.9%Fe/RHS 400 catalyst at 120ºC under dry media conditions with different Limonene:tBHP ratios (20 min reaction, free microwave power, 0.15mgs catalyst)

With regards to the reaction temperature, from Table 9, a value of 150ºC was favoured, since higher temperatures produced over oxidation of carvone, decreasing the selectivity to this compound and at lower temperatures lower conversions were attained.

Temperature (ºC)	Conversion (%)	$S_{carvone}$ (%)
140	45	38
150	60	36
160	70	21

Table 9. Conversions and selectivities of 8.9%Fe 400 catalyst at different temperatures under dry media conditions (limonene:tBHP solution ratio=1:3.5, 20 min reaction time, free microwave power, 0.15mg catalyst)

Based on these results, the parameters chosen for the experiments carried out under liquid conditions were a reaction temperature of 150ºC, reaction times up to 2 h (with reflux attachment), limonene:tBHP solution=1:3.5 (volume ratio), 18 ml total volume, 0.15 g of catalyst. The experimental results obtained under these conditions are presented in Table 10. The main reaction products were the epoxides, carvone and carveol in different amounts. The epoxide found was mainly the endo, with ratios endo/exo+diepoxide close to 2/1+1.

Catalyst/T_{calc} (ºC)	Reaction time min	Conversion %	$S_{epoxides}$ %	$S_{carvone}$ %	$S_{carveol}$ %
Blank 14mL decane	30	5	91	9	0
	60	5	86	14	0
	90	6	85	15	0
	120	6	84	16	0
Silica Evonik	120	6	81	19	0
	30	12	62	24	14
RHS	60	16	50	27	23
	90	22	47	29	24
	120	22	45	31	24
	30	16	74	15	11
RHS HNO_3 400	60	23	59	19	22
	90	33	55	24	21
	120	35	49	30	21
	30	16	69	31	0
RHS HNO_3 600	60	18	55	31	14
	90	24	50	34	16
	120	25	43	35	22
	30	17	76	14	10
4.8%Fe/RHS 400	60	23	72	16	12
	90	35	67	18	15
	120	37	55	26	19
	30	16	77	13	10
4.8%Fe/RHS 600	60	20	69	18	13
	90	29	61	22	17
	120	30	54	27	19
	30	16	88	12	0
8.9%Fe/RHS 400	60	25	68	19	13
	90	41	64	21	15
	120	43	58	23	19
	30	19	73	16	11
8.9%Fe/RHS 600	60	21	68	18	14
	90	31	63	20	17
	120	33	54	24	22
8.9%Fe/RHS 400[c]	30	5	75	20	5
	60	9	70	21	9
	90	20	65	22	10
	480*	22	55	20	10

[c] Conventional heating (* Other products found, mainly carvacrol)

Table 10. Conversions and selectivities under liquid conditions. (Limonene:tBHP ratio=1:3.5, 0.15g catalyst, 150ºC, reflux.

Repeat experiments with fresh catalysts showed a 1-2% difference in conversions and 2-3% in selectivities in both the dry media and liquid phase conditions. It can be seen that in the absence of catalyst, a conversion of ca. 5% after 30 min of reaction was reached and maintained throughout the experiment, with a selectivity of 91% to limonene oxides and 9% carvone. RHS gave a 12% conversion after 30 min, reaching 22% at 90 min with no further increase by the final reaction time of 2 h. The selectivity to epoxides, after 30 min was higher than 60%, decreasing to *ca* 45% by the end of the reaction, with increasing amounts of carvone and carveol. This reactivity was as expected, due to the intrinsic basicity of the oxides contained in this silica (see Figure 14).

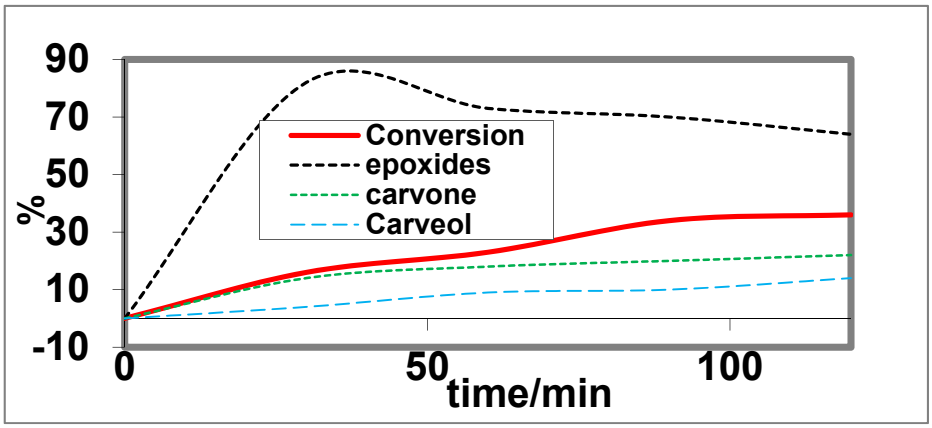

Figure 14. Conversions and selectivities of 8.9%Fe/RHS with orange peel oil, under the conditions shown in Table 10.

The reactivity of RHS HNO_3 400 was higher than that of RHS, reaching *ca* 34% after 90 min, in agreement with the higher basicity, surface area and pore volume of the former. The reactivity of RHS HNO_3 400 was higher than that of RHS HNO_3 600, for the same reasons. The activity of commercial silica Aerosil Evonik, chosen for its similar textural properties (91 m^2g^{-1}), to RHS but with no basic oxides content was practically that observed with no catalyst, showing the importance of basic sites on the reaction. With regards to the catalytic activity of the Fe-containing catalysts, higher conversions were reached with those catalysts prepared with greater amounts of iron and lower calcination temperatures, as seen in the dry media results, in agreement with their higher amounts of basic sites (Figure 13) and better accessibility, as shown in the study of their textural properties (Table 7).

The low reaction times needed in this work due to optimisation of the catalysts and dielectric activation avoids the formation of undesired products, such as polymers sometimes found in the oxidation of limonene at longer reaction times [24]. These workers find one of the technological advantages to be that, since the final mixtures contain high concentrations of valuable oxygenated products of interesting organoleptic properties, they can be used directly, for example in fragrance compositions where separation is unnecessary.

As in Menini´s work [29] at ca. 40% conversion, the reactions become stagnant. Addition of fresh catalyst to the mixture of the substrate and the products does not promote further conversion of the substrate, which seems to indicate that the products accumulated are probably acting as radical scavengers. No iron leaching occurred under the reaction conditions and the catalysts could be recovered by thorough washing with decane and reused at least three times with no appreciable loss of activity. Under the conditions used in Table 10, the behaviour of catalyst 8.9%Fe 400 was determined:

1. adding a small amount (70 μg) of radical scavenger hydroquinone
2. with conventional heating
3. with orange oil, instead of limonene

Addition of hydroquinone greatly decreased the activity, down to that found with no catalyst, indicating the radical nature of the reaction. Under conventional heating after 2 h refluxing, only 22% conversion was reached with 55% selectivity to the epoxides, 20% to carvone, 10% to carveol and 15% to carvacrol, the latter compound due to the extended oxidation under the conditions used. When orange oil was used (Figure 14), the compounds present other than limonene (myrcene, alpha pinene, beta pinene, linalool and decanal) were recovered unreacted and thus the results were promising, especially bearing in mind its lower price, compared to commercial limonene.

Comparing the results obtained here with some from the literature, it can be seen that optimised mixed oxides of iron, cobalt and manganese manage to convert 0.5 ml of limonene after 7 h with an oxygen atmosphere, whereas in this work 1.6 ml limonene were converted with tBHP in 1.5 h. As in our work, these authors obtained as products limonene epoxides, carvone and carveol, with selectivity towards limonene oxide, although the presence of cobalt in the composition of those catalysts had a negative influence on their environmental impact [30,31]. Similar conversions were found with V_2O_5/TiO_2 and tBHP. Again, vanadim pentoxide is more toxic than the iron oxide used in our work. Furthermore, limonene glycol and polymers decrease the selectivities to the desired compounds in that work [32]. Laborious and time consuming preparation and optimisation of synthetic hidrotalcites with immobilised palladium and copper in their compositions achieve similar conversions and selectivities to those found here, however reaction times up to 6 h were required in that case and palladium and copper, although quite reactive, are not very environmentally friendly [33].

The main advantage of our process is that the renewable raw materials used for the preparation of the catalysts, with adequate design, can give rise to catalysts that can compete with synthetic ones, prepared usually in more expensive and time consuming ways and therefore less environmentally friendly [34].

4. The use of agricultural residues to improve the textural characteristics of structured solids to decontaminate effluents

Atmospheric contamination from industrial processes that contain VOCs which lead to the formation of photochemical smog is of great important with respect to air quality. The most

usual remedy for this type of pollution are the so called "end of pipe" methods in which catalysts, adsorption beds or a combination of the two are employed. When large volumes of gas are to be treated, the conformation of the catalysts into open channel monoliths or extrudates is a necessity to avoid or reduce the pressure drop across the catalytic bed. However, if incorporated catalysts are used due to their robust nature and abrasion resistance a reduced activity compared to powder catalysts of similar composition is generally encountered due to diffusion limitations of the gas to be treated into the conformed catalyst. This limitation can be reduced by controlling the texture, surface area and porosity, of the incorporated catalyst.

Toluene was chosen as a typical aromatic VOC to be eliminated by its total oxidation from a spiked air stream. The subproducts from the rice industry chosen to modify the physical characteristics of the conformed catalysts were rice husk ash (RHA), from burning the husks to produce electricity, with the added advantage of drastically reducing the volume of this residue, and rice bran (Bran) that is separated from the rice grain during the whitening process. The Bran is a Pore Generating Agent (PGA) that during the firing of the extruded green body at 500°C to form the conformed ceramic is burnt out with the subsequent increase in the overall porosity of the structure. Whilst the RHA was used to both modify the porosity of the structure and hopefully increase the mechanical strength of the ceramic due to its high silica content [35].

Different compositions and textural properties can be achieved by careful design of the structured solids prepared using rice production wastes (rice husk ash and rice bran). Optimisation of these processes lowers the temperature and therefore the economic expenditure for decontamination of effluents spiked with toluene, chosen as standard for comparison purposes and for being a classical example of a VOC. The textural developement of the solids is a key point to change their behaviour, where the use of rice wastes are a convenient, cheap and ecologic way to improve the activities of the final materials.

The clay used as the agglomerating agent and as the final support for the catalyst was α-sepiolite (Sep), due to its exceptional rheological properties that allow extrusion of the paste produced by mixing with water [36] and the formation of a stable ceramic body with an acceptable strength when heat treated at temperatures above 330°C. Iron nitrate was used as the precursor to the catalyst due to its low cost, toxicity and environmental impact [37]. Four incorporated catalysts [38] were prepared in which the iron to sepiolite ratio was maintained constant but different amounts of Bran and RHA were also incorporated into the original paste before mixing, extrusion and firing at 500°C. Heat treatment at 500°C was chosen since at this temperature the sepiolite forms a ceramic structure that binds all of the other components in the extruded paste. Also this temperature is sufficient for the decomposition of the iron salt to iron oxide which is complete by 200°C, and the thermal decomposition of the Bran. The catalytic activity studies were carried out by passing an air flow spiked so as to contain 100 ppm of toluene through the catalyst bed with a Gas Hourly Space Velocity (GHSV) similar to that expected for the decontamination of an industrial effluent stream. The temperature of the catalyst bed was raised from ambient to 500°C in a number of steps,

maintaining each for a period of 20 min to ensure that the result was in equilibrium and monitoring the destruction of the organic by the use of a flame ionisation detector. The gas balance was confirmed by the amount of CO_2 produced, monitored by infra red spectroscopy.

The original compositions of the green bodies and the textural, mechanical and catalytic activities of these materials after heat treatment at 500°C to produce the conformed ceramic catalyst as a solid extrudate with a diameter of 3 mm are collated in Table 11.

Sample	Composition Sep/Fe/Bran/RHA Parts by Weight	Crushing Strength MPa	Surface Area m^2g^{-1}	Pore Volume cm^3g^{-1}	Catalytic Activity T_{50} °C
1	17/1/0/0	18.3	143	0.576	382
2	17/1/2/0	13.8	140	0.734	350
3	17/1/0/2	19.0	125	0.656	377
4	17/1/2/2	15.8	124	0.797	343

Table 11. Compositional and Textural Characteristics of the catalysts heat treated at 500°C.

From the results presented in Table 11 it may be observed that the mechanical strength of the materials was reduced by the incorporation of Bran into the original paste before extrusion and its subsequent removal by heat treatment at 500°C comparing the result obtained with samples 1 and 2 and that of samples 3 and 4. This was to be expected since with the removal of the PGA on firing at 500°C there is a significant increase in the total pore volume. The mechanical strength of brittle ceramics is related to both the total pore volume and the pore size distribution [39] where an increase in the pore volume or the size of the pores is detrimental to the strength development. From the porosimetry curves presented in Figure 15 it may be seen how the thermal decomposition of the Bran led to both an increase in the total pore volume and a shift to wider pores. Thus, sample 1 had a monomodal pore size distribution curve with practically the whole pore volume located in pores of less than 200 nm. When Bran was incorporated and subsequently burnt out of the conformed material there was a 27% increase in the total pore volume located in the pores between 100 nm and 1 μm.

With the incorporation of RHA the most obvious change in the porosity of sample 3 compared to that of sample 1 was the development of a bimodal curve with the pores close to 900 nm being due to the particle size of the RHA. The slight reduction in the porosity in pores up to about 100 nm was due to the reduction in the amount of Sep per gramme of material. The effects of the incorporation of both RHA and Bran may be seen by comparing the curves obtained with sample 3 with that of sample 4. The curves were similar up to about 100 nm then their was a gradual increase in the pore volume that reached about 21% and a shift in the diameter of the wider pores to approximately 1.5 μm.

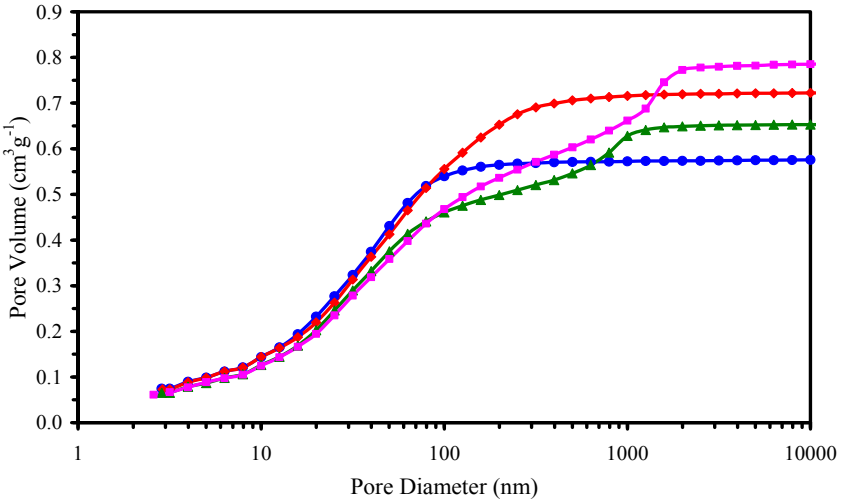

Figure 15. Cumulative pore volume curves for samples heat treated at 500°C: 1 ●, 2 ♦, 3 ▲ and 4 ■.

The catalytic oxidation activity of the four samples is presented in Figure 16 where it may be seen that the least active was that based on sample 1 which had the lowest total pore volume and narrowest pores. With the introduction of Bran into the original composition and its subsequent removal by heat treatment at 500°C which led to a significant increase in both the pore volume and the connectivity the temperature at which 50% of the toluene was decomposed (T_{50}) was reduced by 32°C. For sample 3, although the pore volume and width of the largest pores was increased, which should have lead to less diffusion limitation, the T_{50} was only reduced by 5°C. The highest catalytic activity was found with sample 4 which had the

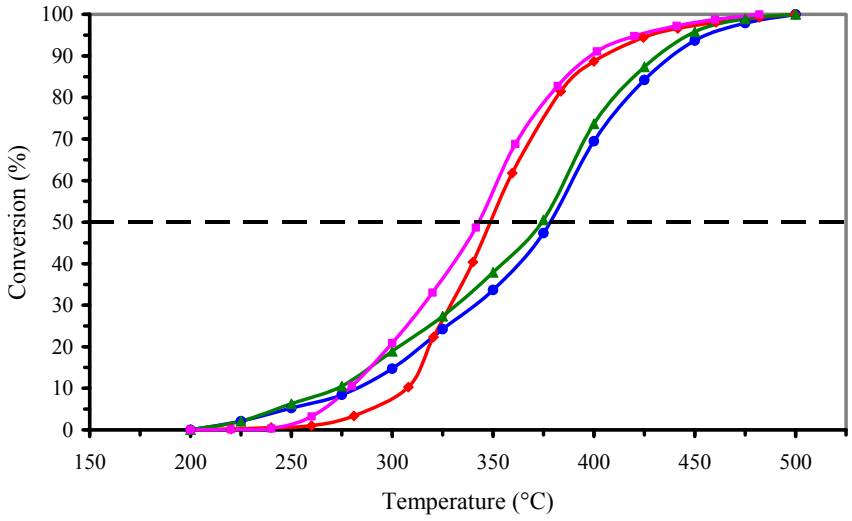

Figure 16. Catalytic activity curves for samples heat treated at 500°C: 1 ●, 2 ♦, 3 ▲ and 4 ■.

advantage of the highest pore volume and the widest pore diameters due to the presence of both Bran and RHA in the original composition. The T_{50} was reduced by 39°C and the material also had a respectable mechanical strength due to the incorporation of the RHA.

5. Preparation of renewable biocompatible scaffolds for bone replacement therapy

Under this heading we present how agricultural wastes have been analysed, modified and changed in order to have properties similar to bone growth scaffolds. SEM micrographs (Figure 17) allow the observation of the porous nature of the inorganic skeleton that remains after the treatment of the waste, and its similarity to bone.

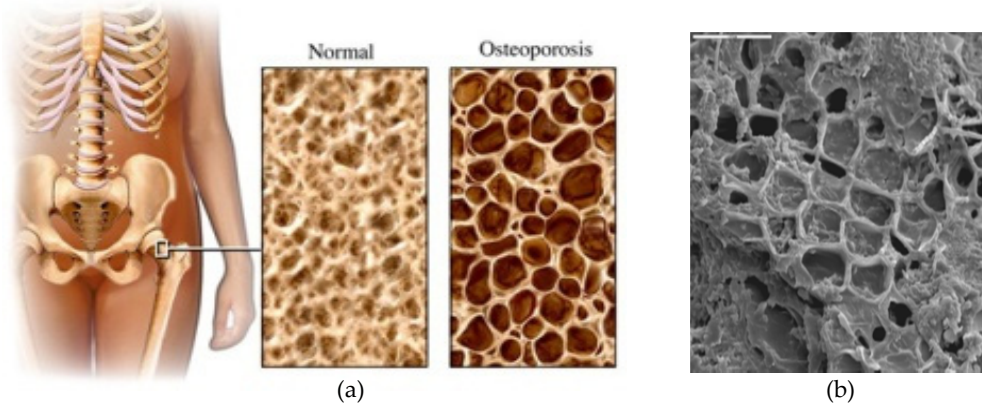

Source a: http://blogdefarmacia.com/tipos-de-osteoporosis/ b: Bioecomaterial (from our own production)

Figure 17. Scanning electron micrograph of treated beer bagasse (scale bar 20 μm) and similarity with bone structure

XRD analysis of these materials show tricalcium phosphate and calcium silicate of structure and composition similar to the synthetic materials presently used in bone and tooth replacement (Figure 18). These materials have proven to be biocompatible and capable of promoting bone growth as confirmed by similar growth rates in vitro of osteoblasts to those of hydroxyapatite used as standard.

It is estimated that approximately a million bone grafts are performed each year to treat bone defects resulting from trauma and diseases in the United States. Various strategies have been used to solve this problem. Autografts are used to treat these defects, but available bone can be inadequate and difficult to shape and obtain. Allografts and xenografts must be processed to eliminate the risk of transmission of live viruses [40]. These difficulties have been the impetus for research into a variety of bone grafting materials.

Bone tissue engineering techniques have become an expanding research area in regenerative medicine. Bone and tooth replacement require materials that act as scaffolds or artificial extra-cellular matrix, directing tissue formation and allowing the transport of biological

nutrients to restore the structure and function of damaged tissues. These materials, which require tailored porosity, surface chemistry, and mechanical strength, are typically produced from animal bone, organic oil-derived polymers, inorganic materials, or complex mixtures of all the above [41]. Figure 19 includes the mercury intrusion porosimetry results for a beer bagasse derived bioecomaterial.

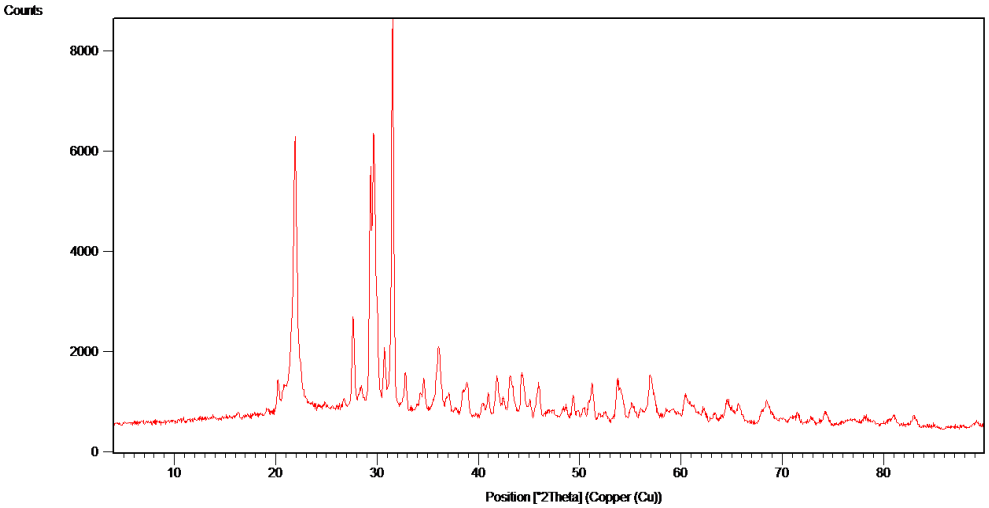

Figure 18. X-ray diffraction of beer bagasse based Bioecomaterial

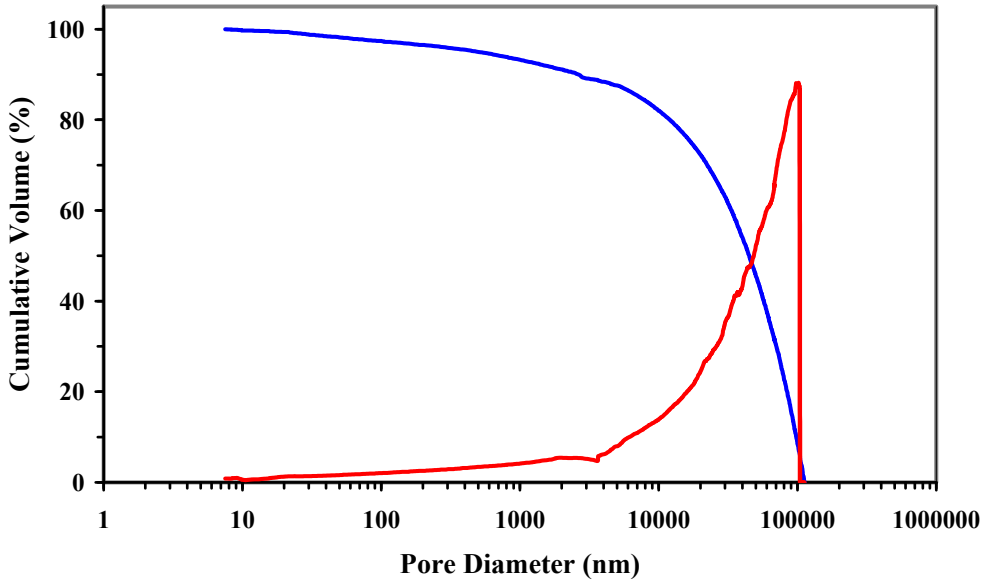

Figure 19. Cumulative Pore Volume (blue line) and pore size distribution (red line) of beer bagasse based bioecomaterial.

The SEM image of the treated beer bagasse (Figure 17b) displayed pores of about 10μm. However, from the mercury intrusion porosimetry curve presented in Figure 19 it may be appreciated that a continuously increasing curve was observed from the largest pores down to those at the physical limit of this technique (4 nm). Thus, although the cumulative intruded volume in the largest pores was due to filling of the intraparticulate space, while at diameters below 10 μm the porosity must be due to the interparticulate porosity. However, what is most important from this figure is that the porosity between the particles and within them formes a continuous network that favours cell growth when used as a scaffold for bone regeneration.

Materials used as bone substitutes need to embrace several important requirements: i) biocompatibility; ii) osteoinduction and osteopromotion, iii) porosity, iv) stability under stress, v) resorbability and degradability, vi) plasticity, vii) sterility and viii) stable and long-term integration of implants [42]. All these requirements serve as a basis for effective long-term tolerance in bone replacement therapies [43].

The first approach in the selection of a suitable scaffold for bone regeneration is the evaluation of its in vitro cytotoxicity using appropriate cell lines in culture, such as osteoblasts. Thereby, we can determine the biocompatibility of each scaffold under study. A good biocompatibility could be expected from materials whose physicochemical properties promote cell adhesion and differentiation into mature osteoblasts.

In the present study we aimed to develop scaffolds for bone regeneration obtained from agricultural wastes from several crops. These materials have proved to be good replacement candidates for use as biomaterials for the growth of osteoblasts and could be used in bone replacement therapies.

In this study, beer bagasse, a low-cost waste material from beer production, was employed as a renewable raw material that was tailored for use as biocompatible scaffolds for osteoblast growth, given its structure and composition [44-46]. To the best of our knowledge this is the first time that agricultural waste has been modified to produce solids that can act as scaffolds for tissue regeneration.

To study cell adhesion to the materials, their biocompatibility and efficiency for bone growth, MC3T3-E1, an osteoblast-like cell line, was chosen because they are well characterised for modelling endogenous osteoblasts [47]. A commercial synthetic scaffold, hydroxyapatite (HA) nanopowder (B200 nm) from Sigma Aldrich, was used for comparison purposes.

The osteoblastic cells were seeded onto material-coated plates in DMEM-10%FBS and allowed to adhere for 2 h at 37ºC in a 5% CO_2 atmosphere. Plates were then washed with phosphate-buffered based saline solution (PBS) to remove non-adherent cells. Adherent live cells were quantified using the live/dead viability assay kit (Molecular Probes [40]). The number of live adhered cells was evaluated 2h after seeding by fluorescence microscopy, counting at least 10 representative fields per well. The cell adhesion process was studied after 2h of incubation at 37ºC. The adhesion of MC3T3E1 cells to the various materials

evaluated is shown in Figure 20. As can be seen, the number of osteoblast cells which adhered to the materials derived from beer bagasse was comparable to that of the commercial material used as control (HA). The cell adhesion rate was even higher in the case of sample BB47. However, the adhesion of MC3T3E1 cells to the materials was slightly lower than that on plastic, especially for cells seeded on HA and BB48. Assuming 100% as the rate of cell adhesion for the commercial material (HA), those for BB47, BB48 and BB410 were found to be 141.5%+/- 6.1, 92.5%+/-7.4 and 118.1%+/-5.8, respectively. Thus, confirming similar adhesion rates for the studied materials, demonstrating that they possess an appropriate porosity to allow cell adhesion.

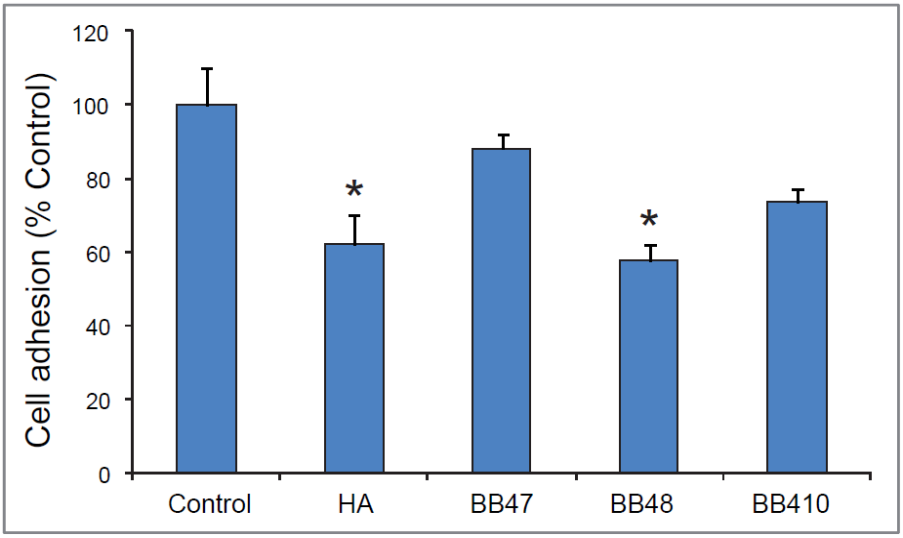

Figure 20. Adhesion of MC3T3E1 cells. Cells were plated on a plastic control dish (Control) and on plates coated with the control material (HA) and with materials derived from beer bagasse (BB47, BB48, BB410). Cells were incubated for 2h at 37ºC. Then, adherent live cells were quantified as described in the text. Results are expressed as a percentage of the control (cells seeded on plastic plates). Data represent mean+/-S.E.M. of three independent experiments. ($p<0.05$, ANOVA, post-hoc Tukey HSD test, * vs. Control).

The biocompatibility of the materials derived from beer bagasse, was assessed with the same MC3T3-E1 cells after different periods of exposition, comparing the results to those obtained with the commercial material HA and to regular tissue culture polystyrene plates, used as controls. The viability of MC3T3-E1 cells growing on plastic plates, BB47, BB48, BB410 and the commercial material HA was determined at one, three and seven days after seeding by the live/dead viability assay [48], to distinguish dead cells (red) from live ones (green), as observed by inverted fluorescence microscopy (Figures 21 and 22).

Calculating the percentage of live cells over total cells (live cells plus dead cells), a high cell viability rate was observed for all scaffold materials produced from beer bagasse, similar to that of the commercial product HA and the control cell culture plastic plates (Figure 21).

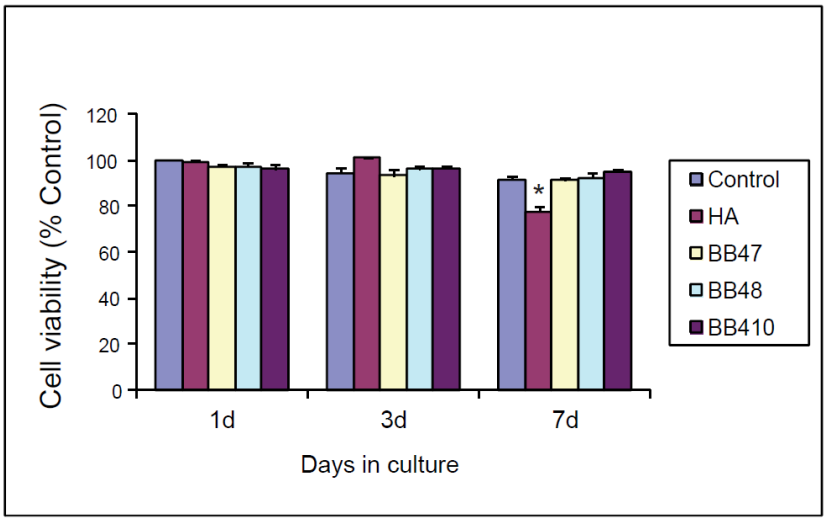

Figure 21. MC3T3-E1 cell viability after 1, 3 and 7 days growing on plastic plates or on plates coated with HA, BB47, BB48 and BB410. Cell viability was evaluated by live/dead viability assay kit. Data represent mean+/-S.E.M. of three independent experiments. ($p<0.05$, ANOVA, post-hoc TukeyHSD test, * vs. Control).

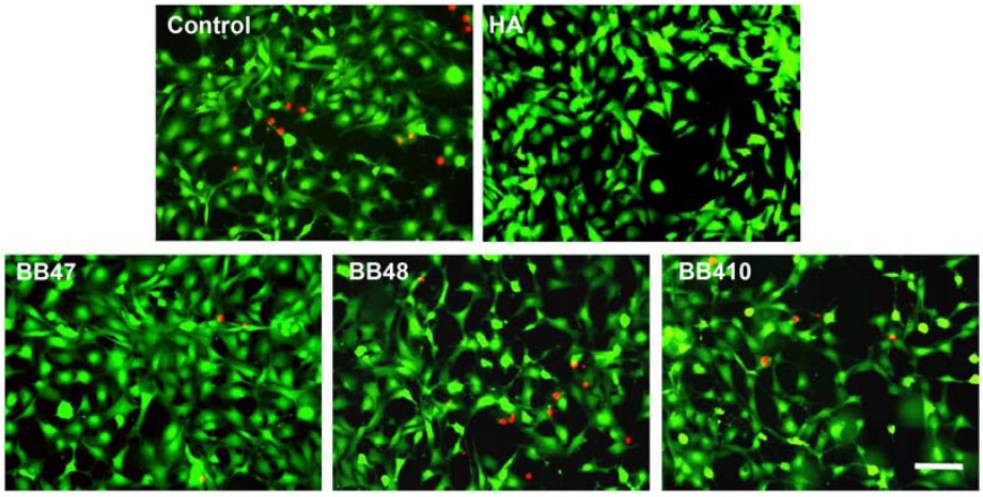

Figure 22. Fluorescence microscopy images showing MC3T3-E1 cells growing on different materials 3 days after seeding and stained with Live (green)-Dead (red) viability assay kit. Scale bar: 100μm.

None of the materials analysed resulted in a reduction of cell viability at any time points, more than 90% of the cells growing on these materials remained viable over the whole evaluation period. Only cells growing on HA for 7 days showed a significant reduction in the rate of cell viability.

Since bone formation is a lengthy process, the most relevant aspect is that even after seven days of culture, all materials displayed similar biocompatibilities rates to those observed on the commercial sample and the plastic plates.

In summary, murine-derived osteoblastic cells (MC3T3-E1) actively adhere to the beer bagasse-derived materials, with no significant changes in cell viability of cells growing on these materials compared to those observed with either the commercial material or the cells seeded directly onto plastic plates. Such characteristics are desired in dental and orthopaedic prostheses [49].

We conclude that our renewable raw material (RRM) are scaffolds that have the right characteristics to support adhesion and survival of the osteoblast-derived cell line MC3T3E1, strongly suggesting that they could be employed in oral and/or bone tissue regeneration.

6. Conclusions

1. Agro-industrial wastes are a renewable source of many solid and liquid substances and furthermore, their use leads to a reduction in environmental hazards. These wastes are an inexhaustible and sustainable source of materials and substances in a biorefinery based economy that is constantly gaining interest in industrial sectors, especially because the actual petroleum based will come to an end.
2. Some agricultural wastes, can be used as catalysts for production of fine chemicals. For example, silica prepared from rice husk, with a lamellar structure, basicity due to oxides from its natural origin and unusual high density, can act both as support and catalyst for the oxidation of limonene. Also, sustainable chemicals can be produced from agricultural wastes.
3. The use of agricultural wastes allows the production of extrudates that can be employed to optimise cleaning of contaminated effluents. The catalytic activity of conformed catalysts may be significantly enhanced by the use of low cost sub-products and residues from the rice production industry. Rice bran is a useful PGA that improves the connectivity of the porous matrix in these incorporated catalysts while the RHA both improves the strength development of the ceramic body while also improving the texture and thus reducing the diffusion limitations of the gas to be treated into the porous structure of the catalyst.
4. Some waste derived solids, after the appropriate pretreatment, can be used for bone growth. The biocompatibility of some modified agro-industrial wastes has shown to be interesting in their use in fields like release of medicines, supports for enzymes and food supplements. Recent studies “in vivo” are showing promising results for these materials as economical sustainable scaffolds to be used in tissue engineering.

Author details

M.A. Martin-Luengo, E. Sáez Rojo, A.M. Martínez Serrano,
M. Diaz, L. Vega Argomaniz, L. Medina Trujillo and S. Nogales
Department of New Architectures, Institute of Materials Science of Madrid, CSIC, Spain

M. Yates, F. Plou, E. Sáez Rojo, M. Diaz,
L. Vega Argomaniz, S. Nogales and R. Lozano Pirrongelli
Institute of Catalysis and Petroleochemistry, CSIC, Spain

M. Ramos and A.M. Martínez Serrano
Centre for Biomedical Technology, Polytechnical University of Madrid, Spain

J.L. Salgado
AIZCE Technical Committee, Interprofesional Asociation of Juices and Citric Concentrates

J.L. Lacomba and and A. Civantos
Institute of Biofunctional Studies, Complutense University of Madrid, Madrid, Spain

G. Reilly
Department of Materials Science and Engineering, Kroto Research Institute, Broad Lane, University of Sheffield, Sheffield, United Kingdom

C. Vervaet
Laboratory of Pharmaceutical Technology, Gent, Belgium

7. References

[1] Kem-Laurin K, (2012) Approaches to A Sustainable User Experience User Experience in the Age of Sustainability, Pages 31-68.

[2] Mahesh K, Utkarsh Ravindra M, Adinpunya M (2012) Rapid separation of carotenes and evaluation of their in vitro antioxidant properties from ripened fruit waste of Areca catechu – A plantation crop of agro-industrial importance. Ind. Crops and Products, 40: 204-209.

[3] Brady NC, Weil, RR (1999) The Nature and Properties of Soils (12th ed), Prentice Hall, Upper Saddle River, New Jersey.

[4] Notarnicola B, Kiyotada H, Curran MA, Huisingh D (2012) Progress in working towards a more sustainable agri-food industry. J. of Cleaner Production, 28: 1-8.

[5] Karlen DL, Ditzler CA, Andrews SS (2003) Soil quality: why and how? Geoderma, 114: 145-156.

[6] Cogo SLP, Chaves FC, Schirmer MA, Zambiazi RC, Nora L, Silva JA, Rombaldi CV (2011) Low soil water content during growth contributes to preservation of green colour and bioactive compounds of cold-stored broccoli (Brassica oleraceae L.) florets. Postharvest Biology and Technology, 60:158-163.

[7] Pérez-Balibrea S, Moreno DA, García-Viguera C (2011) Improving the phytochemical composition of broccoli sprouts by elicitation. Food Chemistry, 129: 35-44.
[8] Vallverdú-Queralt A, Medina-Remón A, Casals-Ribes I, Lamuela-Raventos RM (2012) Is there any difference between the phenolic content of organic and conventional tomato juices? Food Chemistry, 130: 222-227.
[9] Salgado JL, AIZCE Technical Committee (Interprofessional association of Citric Juices and concentrates of Spain).
[10] Martin-Luengo MA, Yates M, Martínez Domingo MJ, Casal B, Iglesias M, Esteban M, Ruiz-Hitzky E (2008) Synthesis of p-cymene from limonene, a renewable feedstock. Appl. Catal. B: Env. 81: 218-224.
[11] Aschmann SM, Arey J, Atkinson R (2011) Formation of p-cymeme from OH + γ-terpinene: H-atom abstraction from the cyclohexadiene ring structure. Atmospheric Env. 45: 4408-4411.
[12] Yadav GD, Purandare SA (2007, Vapor phase alkylation of toluene with 2-propanol to cymenes with a novel mesoporous solid acid UDCaT-4, Microp. and Mesop. Materials, 103: 363-372.
[13] Rouquerol F, Rouquerol J, Sing K.S.W (1999) Adsorption by Powders and Porous Solids: Principles, Methodology and Applications.
[14] Lavalley JC (1996) Infrared spectrometric studies of the surface basicity of metal oxides and zeolites using adsorbed probe molecules, Catal. Today 27: 377-401.
[15] Leyva C, Ancheyta J, Travert A, Maugé F, Mariey L, Ramírez J, Rana MS (2012) Activity and surface properties of NiMo/SiO_2–Al_2O_3 catalysts for hydroprocessing of heavy oils. Appl. Catal. A: Gen. 425–426: 1-12.
[16] Fernandes C, Catrinescu C, Castilho P, Russo PA, Carrott MR, Breen C, (2007) Catalytic conversion of limonene over acid activated Serra de Dentro (SD) bentonite. Appl. Catal. A: Gen. 318: 108-120.
[17] Catrinescu C, Fernandes C, Castilho P, Breen C (2006) Influence of exchange cations on the catalytic conversion of limonene over Serra de Dentro (SD) and SAz-1 clays: Correlations between acidity and catalytic activity/selectivity. Appl. Catal. A: Gen 311: 172-184.
[18] Schneider RCS, Baldissarelli VZ, Martinelli M, von Holleben MLA, E.B. Carama EB (2003) Determination of the disproportionation products of limonene used for the catalytic hydrogenation of castor oil. J. Chromatogr. A 985: 313-319.
[19] Martin–Luengo MA, Pajares JA, González TejucaL (1985) Particle size determination of palladium supported on sepiolite and aluminum phosphate. J. of Colloid and Interface Sci. 107: 540-546.
[20] Oh S-T, Kim M-S, Choa Y-H, Kim KH, Lee S-K (2012) Preparation of Fe–50 wt.% Co nanopowders by calcination and hydrogen reduction of nitrate powders. Microelectronic Eng. 89: 97-99.

[21] Xu W, Liu X, Ren J, Liu H, Ma Y, Wang Y, Lu G (2011) Synthesis of nanosized mesoporous Co–Al spinel and its application as solid base catalyst. Microp. and Mesop. Materials 142: 251-257.

[22] Gervasini C, Messi P, Carniti A, Ponti N, Ravasio F, Zaccheria F (2009) Insight into the properties of Fe oxide present in high concentrations on mesoporous silica. J. of Catal. 262: 224-234.

[23] Zhao C, Gan W, Fan X, Cai Z, Dyson PJ, Kou Y. (2008) Aqueous-phase biphasic dehydroaromatization of bio-derived limonene into *p*-cymene by soluble Pd nanocluster catalysts. J.Catal. 254: 244-250.

[24] Lee OC, Oh Y-G. and S-G (2009) Synthesis and characterization of hollow silica microspheres functionalized with magnetic particles using W/O emulsion method. Coll. and Surf. A: Physicochem. and Eng. Aspects 337: 208-212.

[25] Baraton M, X. Chen X, Gonsalves KE (1997) Ftir study of a nanostructured aluminum nitride powder surface: Determination of the acidic/basic sites by CO, CO_2 and acetic acid adsorptions. Nanostr. Mater. 8: 435-445.

[26] Ross PF, Busca G, Lorenzelli V, Lion M, Lavalley C (1988) Characterization of the surface basicity of oxides by means of microcalorimetry and fourier transform infrared spectroscopy of adsorbed hexafluoroisopropanol. , J. Catal. 109: 378-386.

[27] Oliveira P, Machado A, Ramos AM, Fonseca I, Fernandes FMB, Botelho do Rego AM, VitalJ (2009) MCM-41 anchored manganese salen complexes as catalysts for limonene oxidation Microp. and Mesop. Materials 120: 432-440

[28] Martin-Luengo MA, Yates M, Diaz M, Saez Rojo E, Gonzalez Gil L (2011) Renewable fine chemicals from rice and citric subproducts: Ecomaterials. Appl. Catal. B: Env. 106: 488-493.

[29] Menini L, Pereira MC, Parreira LA, Fabris JD, Gusevskaya EV (2008) Cobalt- and manganese-substituted ferrites as efficient single-site heterogeneous catalysts for aerobic oxidation of monoterpenic alkenes under solvent-free. J. Catal. 254: 355-364.

[30] Menini L, Pereira MC, Parreira LA, Fabris JD, Gusevskaya EV (2008) Cobalt- and manganese-substituted ferrites as efficient single-site heterogeneous catalysts for aerobic oxidation of monoterpenic alkenes under solvent-free conditions. J. Catal. 254:355-364.

[31] Robles-Dutenhefner PA, da Silva MJ, Sales LS, Sousa EMB, Gusevskaya EV (2004) Solvent-free liquid-phase autoxidation of monoterpenes catalyzed by sol–gel Co/SiO_2. J. Mol. Catal. A: Chem. 217: 139-144.

[32] Oliveira P, Rojas-Cervantes ML, Ramos AM, Fonseca IM, Botelho do Rego AM, Vital J (2006) Limonene oxidation over V_2O_5/TiO_2 catalysts. Catal. Today 118: 307-314.

[33] Bussi J, López A, Peña F, Timbal P, Paz D, Lorenzo D, Dellacasa E (2003) Liquid phase oxidation of limonene catalyzed by palladium supported on hydrotalcites. Appl. Catal. A: Gen. 253: 177-189.

[34] Guidotti M, Ravasio N, Psaro R, Ferraris G, Moretti G (2003) Epoxidation on titanium-containing silicates: do structural features really affect the catalytic performance? J. Catal. 214: 242-250.

[35] Jimmy Nelson Appaturi, Farook Adam, Zakia Khanam (2012) A comparative study of the regioselective ring opening of styrene oxide with aniline over several types of mesoporous silica materials. Microporous and Mesoporous Materials 156:16-21.

[36] Murray HH (1991) Overview — clay mineral applications. Applied Clay Science 5: 379–395.

[37] Kim SC, Shim WG (2008).Influence of physicochemical treatments on iron-based spent catalyst for catalytic oxidation of toluene. Journal of Hazardous Materials 154: 310-316.

[38] Cybulsky A and Moulin JA (1998) Structurated Catalysts and Reactors. Ed. Marcell and Dekker, Inc New York.

[39] Yates M (2006) Application of mercury porosimetry to predict the porosity and strength of ceramic catalyst supports. Particle & Particle Systems Characterization 23: 94-100.

[40] Simon, C.G.; Guthrie, W.F.; Wang, F.W. (2004) Cell Seeding into Calcium Phosphate Cement. J. Biomed. Mater. Res. Part A 68A: 628-639.

[41] Cao, H.; Kuboyama, N. A (2010) Biodegradable Porous Composite Scaffold of PGA/b-TCP for Bone Tissue Engineering. Bone 46: 386-395.

[42] Kolk A, Handschel J, Drescher W, Rothamel D, Kloss F, Blessmann M, Heiland M, Wolff KD, Smeets R (2012) Current trends and future perspectives of bone substitute materials - From space holders to innovative biomaterials. J Craniomaxillofac Surg. (in press, corrective proof, available online 30th Jan)

[43] Horch HH, Sader R, Pautke C, Neff A, Deppe H, Kolk A (2006) Synthetic, pure-phase beta-tricalcium phosphate ceramic granules (Cerasorb) for bone regeneration in the reconstructive surgery of the jaws. Int. J. Oral Maxillofac Surg, 35: 708–713.

[44] Harish Prashanth, K.V.; Tharanathan, R.N (2007) Chitin/Chitosan: Modifications and Their Unlimited Application Potential-an Overview. Trends Food Sci. Technol. 18: 117-126.

[45] Al Seadi, T.; Holm-Nielsen B (2004) III. 2 Agricultural Wastes. Waste Management Series 4:207-215.

[46] Martin Luengo M.A.; Yates M.; Casal B. (2010) Preparation of Biocompatible Materials from Beer Production and Their Uses. Spanish patent PCT/ES2009/070475.

[47] Chen, F.; Ouyang, H.; Feng, X.; Gao, Z.; Yang, Y.; Zou, X.; Liu, T.; Zhao, G.; Mao, T. Anchoring Dental Implant in Tissue-Engineered Bone Using Composite Scaffold: A PreliminaryStudy in Nude Mouse Model. J. Oral Maxillofac. Surg. 2005, 63, 586-595.

[48] Chou YF; Huang W; Dunn JC, Miller TA; Wu BM (2005) The Effect of Biomimetic Apatite Structure on Osteoblast Viability, Proliferation, and Gene Expression. Biomaterials 26: 285_295.

[49] Bertazzo, S.; Zambuzzi, W.F.; da Silva, H.A.; Ferreira, C.V.; Bertran, C.A. Bioactivation of Alumina by Surface Modification: A Possibility for Improving the Applicability of Alumina in Bone and Oral Repair. Clin. Oral Implants Res. 2009, 20 (3), 288-293.